

## Carbonate sealing and its controlling factors: cap rock and inner barrier layers of Yingshan Formation on Tazhong Northern Slope, Tarim Basin

Xiaodong LAN<sup>1,\*</sup>, Xiuxiang LÜ<sup>2,3</sup>

<sup>1</sup>School of Ocean Sciences, China University of Geosciences, Beijing, P.R. China

<sup>2</sup>School of Earth Science, China University of Petroleum, Beijing, P.R. China

<sup>3</sup>State Key Laboratory of Petroleum Resources and Prospecting, Beijing, P.R. China

Received: 12.12.2013 • Accepted: 07.07.2014 • Published Online: 03.11.2014 • Printed: 28.11.2014

**Abstract:** The Yingshan Formation, located on the Tazhong Northern Slope, contains oil- and gas-rich layers with the reserves of about  $700 \times 10^6$  TOE. The high-resistivity inner layers isolate the hydrocarbon bearing zones and form the sequential sets of reservoir bed-seal assemblages in a vertical direction within the Yingshan Formation, which is directly bound above by a micritic carbonate cap rock that is overlain by the 3rd to 5th members of the Lianglitag Formation. The sealing capability of the cap rock and inner barrier layers was evaluated macroscopically and microscopically in terms of the core breakthrough pressure and thin-section identification. The evaluation parameters were extracted from the statistical analysis of drilling and logging data. The 3rd to 5th members of the Lianglitag Formation are more shaly, but the inner barrier layers in the Yingshan Formation are more dolomitic. Argillaceous limestone is more capable of sealing oil and gas zones than micritic limestone. The 3rd to 5th members of the Lianglitag Formation, of which the gamma ray response and core displacement pressure are greater than 20 API and 14 MPa, respectively, provide good sealing with thicknesses of more than 100 m and have better sealing with thickness of more than 200 m. For the same porosity, dolomite has lower coreflood displacement pressure than limestone. The difference in coreflood displacement pressure between the barrier layers and the underlying reservoir bed is 6 MPa, the cutoff value for sealing capability. Carbonate sealing was controlled by early sedimentation and was influenced by late diagenesis. The direct cap rock is dense and has cement content of more than 10%, up to 31%. The reservoir bed has cement content of less than 10%. Generally, the direct cap rock and the inner barrier layers are relatively stable on the lateral distribution.

**Key words:** Carbonate cap rock, displacement pressure, sealing ability, Tazhong Northern Slope, Yingshan Formation

### 1. Introduction

High-quality and undestroyed cap rock is indispensable for oil/gas accumulation. For most of the oil and gas basins in the world, cap rock could be shale, mudstone, halite, gypsum rock, dense limestone, evaporite, or volcanics (Fu et al., 2010). Klemme (1975, 1980) analyzed 334 oil fields around the world and found that shale cap rock accounted for 65%, evaporite for 33%, and limestone for only 2%. Recently, clastic cap rocks have been studied widely (Li et al., 1996; Lü and Fu, 1996; Zhang, 1998; Jiao and Gu, 2004; Lu et al., 2007), and a theoretical system was established to research the cap rock both in macroscopic evaluation and microscopic examination. At the macroscopic level, lithology, thickness, and distribution are investigated (Grunau, 1987; Lü et al., 2000; Zhang and Zhou, 2010). At the microscopic level, 3 types of sealing mechanisms are considered: capillary pressure sealing, overpressure sealing, and hydrocarbon saturation sealing (Watts, 1987;

Cheng et al., 2006; Zhang et al., 2010; Fan et al., 2011; Yu et al., 2011). The parameters involve permeability, coreflood breakthrough pressure and time, average pore throat radius, and clay content. Generally, sealing capability is stronger with high clay content, low porosity, and low permeability.

Carbonate rocks, such as dolomite, limestone, and marl, have high compaction resistance (37.15–44.80 MPa), high hardness (776–1218 MPa), and small plastic coefficient (1.43–1.66) and compression coefficient ( $1.37-3.18 \text{ MPa}^{-1}$ ) (Yang and Zhang, 1994). As a hard and brittle rock, carbonate rock is not considered a good cap rock, because it is easily broken, and altered pores and fractures develop with underground denudation. However, with a complex diagenesis process of compaction, filling, and cementation, carbonate rock could become dense with certain sealing capability (Xu and Zhang, 2001). Especially with the presence of clay, its mechanical properties change

\* Correspondence: lansecup@163.com

to low hardness and high plasticity, and carbonate rock could have good sealing capability. Carbonate cap rocks have been reported worldwide, for which the well-known examples are the Bashkirian dense limestone of the Upper Carboniferous in the Volga-Ural Basin, Russia; the Gzhelian argillaceous limestone of the Carboniferous (Peterson and Clarke, 1983; Alekseev et al., 1996; Proust et al., 1998; Li and Zhu, 2012); the argillaceous dolomite and shale of the Lower Triassic as the cap rock of the Khuff Reservoir in the Persian Gulf Basin (Beydoun, 1988; Kashfi, 1992; Alsharhan and Nairn, 1997); the thin-bed dense limestone of the Cretaceous as the cap rock of oil fields in the Dezful Depression, Iran (Bai, 2007); the dense limestone of the Kalash/Waha Formation as the cap rock of the Nubain/Sarir Formation of the Upper Cretaceous in the Sirte Basin, Libya (Parsons et al., 1980; Macgregor, 1986; Tian et al., 2008); the thin- to medium-thick bed of silty crystalline dolomite as the paleo-oil reservoir of the Middle and Lower Cambrian in Tongshan and Wanshan, Guizhou, China (Mei et al., 2006); the thick-bed (100 m) dense micrite and micritic dolomite of the 4th member of the Leikoupo Formation as the direct cap rock of the Triassic gas reservoir in the western Sichuan Basin (Fan, 2009); and the thin- to medium-thick bed of marl of the 3rd member of the Feixianguan Formation as the direct cap rock of the Triassic gas reservoir in the eastern Sichuan Basin (Qin et al., 2011).

The Tazhong Low Rise is located in the Central Uplift, Tarim Basin, which is the largest petroliferous inland basin in China. Since the discovery of a hundred-million-ton condensate field of the Yingshan Formation in the Lower Ordovician of well block Zhonggu 43, commercial oil and gas flows have been encountered in more than 50 wells, including highly productive wells such as well M21 with 74 t oil/day and 144,000 m<sup>3</sup> gas/day, and well M42 with 45 t oil/day and 94,000 m<sup>3</sup> gas/day. Apparent oil and gas reserves of 700 × 10<sup>6</sup> TOE in the Yingshan Formation could be confirmed and are all sealed by the dense limestone of the Lianglitag Formation and the inner barrier layers in the Yingshan Formation itself. In this study, the sealing capability of these 2 types of carbonate sealing was evaluated, and the evaluation parameters and criteria were established.

## 2. Geological setting

The Tazhong Low Rise, with an area of 27.5 × 10<sup>3</sup> km<sup>2</sup>, is located in the Central Uplift, Tarim Basin. As seen in Figure 1, it is a large complete anticline with several WNW-striking secondary structural zones, where the eastern structure is higher than the western structure and both exhibit a bird-foot shape (Wu et al., 2005; Li et al., 2009). The Tazhong Low Rise is divided into the Northern Slope and Southern Slope by the Central Fault Belt. Two

sets of fault networks developed on the Northern Slope, the thrust faults in the NW direction and strike slip faults in the NE direction (Wu et al., 2012).

In the Tazhong Low Rise, marine carbonate beds developed in the Ordovician, Cambrian, and Upper Sinian. At present, most of the exploration wells are on the Tazhong Northern Slope, but the majority of wells did not penetrate through the Ordovician. The Sangtamu and Lianglitag Formations are in Upper Ordovician series, and the Yingshan and Penglaiba Formations are in Lower Ordovician series (Figure 2). As the high-quality regional cap rock, the Sangtamu Formation is primarily dark gray calcareous mudstone with little siltstone and thinly bedded limestone. The Lianglitag Formation is primarily light gray micrite, biosparite, intrasparite, bindstone, and marl. The Lianglitag Formation can be subdivided into 5 lithologic members, the compact limestone in the 3rd to the 5th members that can be direct cap rock for the Yingshan Formation. The Yingshan Formation is not mostly drilled through on the Northern Slope and consists of limestone, dolomite, and their gradual transitions. The formation is divided into 4 members: the 1st member is primarily composed of intrasparite, the 2nd member is primarily composed of intramicrite and micrite, the 3rd member is primarily composed of dolomitic limestone interbedded with micrite, and the 4th member is primarily composed of dolomitic limestone, limy dolomite, and dolomite. The Yingshan Formation is a large-scale gas-condensate reservoir that is quasi-layer distributed and controlled by weathering crust (Zhou et al., 2006; Yang et al., 2007; Han et al., 2008; Lin et al., 2012). As the direct cap rock, the 3rd to 5th members of the Lianglitag Formation directly control the oil/gas distribution in the Yingshan Formation. Oil/gas exploration shows that the Yingshan Formation has more than one oil/gas pay zone. For example, wells M20 (Figure 3) and M35 indirectly indicate that several barrier layers exist in the Yingshan Formation. The individual barrier layers are as thick as a few meters to tens of meters with some lateral continuity, dense lithology, high resistivity (deep and shallow resistivities are more than 1000 Ω m, as shown in Figure 3), and low permeability. These barrier layers are designated as high-resistivity layers in the following discussion.

## 3. Cap rock characteristics and sealing function

### 3.1. Lithology

The 3rd to 5th Lianglitag members are dense limestone and form the direct cap rock for the Yingshan Formation. The lithology and thickness of drilling cuttings from the 3rd to 5th Lianglitag members in 30 wells (7799 m in total, Figure 4a) was examined and the presence was determined of 56% micrite (4399 m long) (Figure 5a), 32% marl (2499 m long) (Figure 5b), 8% silty crystalline limestone (653



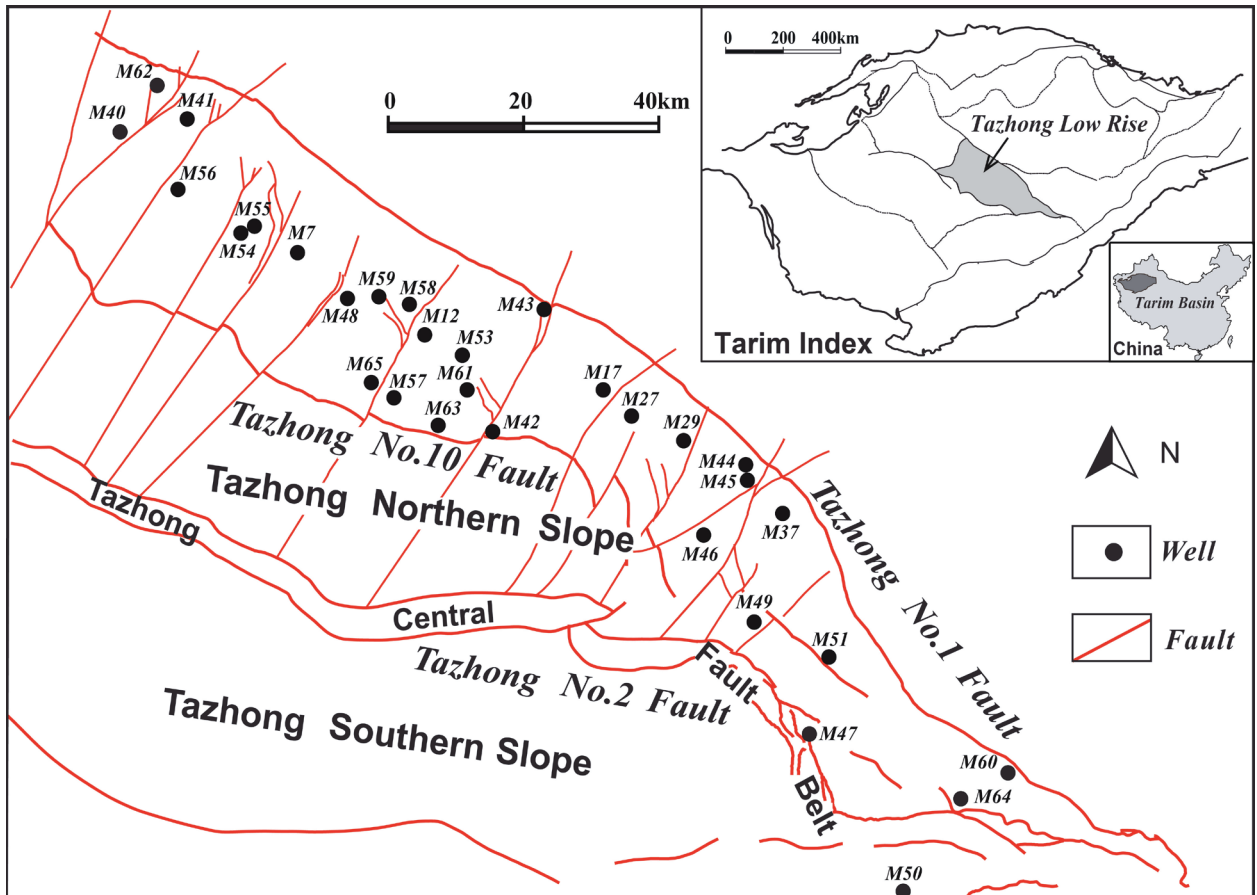


Figure 1. Location and top of structure of the Yingshan Formation on the Northern Slope, Tazhong Low Rise.

m long), 2% argillaceous limestone (121 m long), and a little dolomitic limestone and dolomite. The lithology of high-resistivity layers of the Yingshan Formation in 20 wells was examined (1507 m in total, Figure 4b) and the presence was determined of 55% micrite (832 m long) (Figure 5c), 5% marl (77 m long), 17% silt-size crystalline limestone (262 m long), 2% argillaceous limestone (32 m long), 20% dolomitic limestone (294 m long), and a little dolomite (Figure 5d). These 2 types of carbonate sealing, i.e. the cap rock and high-resistivity barrier layers, on the Tazhong Northern Slope are primarily micrite. The 3rd to 5th members of the Lianglitag Formation are more shaly, and high-resistivity layers in the Yingshan Formation are more dolomitic.

### 3.2. Thickness and distribution

The 3rd to 5th members of the Lianglitag Formation cover the whole Tazhong Northern Slope and its thickness reduces from about 300 m at the Tazhong No. 1 Fault belt (279 m in well M43) to several meters at the Central Fault Belt. The cap rock in the Tazhong No. 10 structural belt is nearly 200 m thick; for example, it is 190 m in well M19 and 247 m in well M42. Additionally, the 4th to 5th

members are lost in most parts of the western Tazhong Low Rise and form the thicker cap rock in the east and thinner in the west (Figure 6). The 3rd to 5th members of the Lianglitag Formation are 100 m to 200 m thick on average, e.g., 114 m in well M55 and 115 m in well M9. Its thickness in the east is more than 300 m with a maximum of more than 800 m, e.g., 306 m in well M27, 522 m in well M49, and 854 m in well M60. The dense limestone is widely distributed with a large thickness and makes a good sealing for the oil/gas zones in the Yingshan Formation.

As seen in the fence diagram in Figure 6, there are 6 high-resistivity layers with stable distribution within the 1st and 2nd members of the Yingshan Formation: 1) the upper section of the 1st member, denoted Y1-G1; 2) the lower section of the 1st member, denoted Y1-G2; 3) the upper-1 section of the 2nd member, denoted Y2-G1; 4) the upper-2 section of the 2nd member, denoted Y2-G2; 5) the upper-3 section of the 2nd member, denoted Y2-G3; and 6) the lower section of the 2nd member, denoted Y2-G4. Note that the Yingshan Formation was denuded gradually from the Tazhong No. 1 Fault Belt to the Central

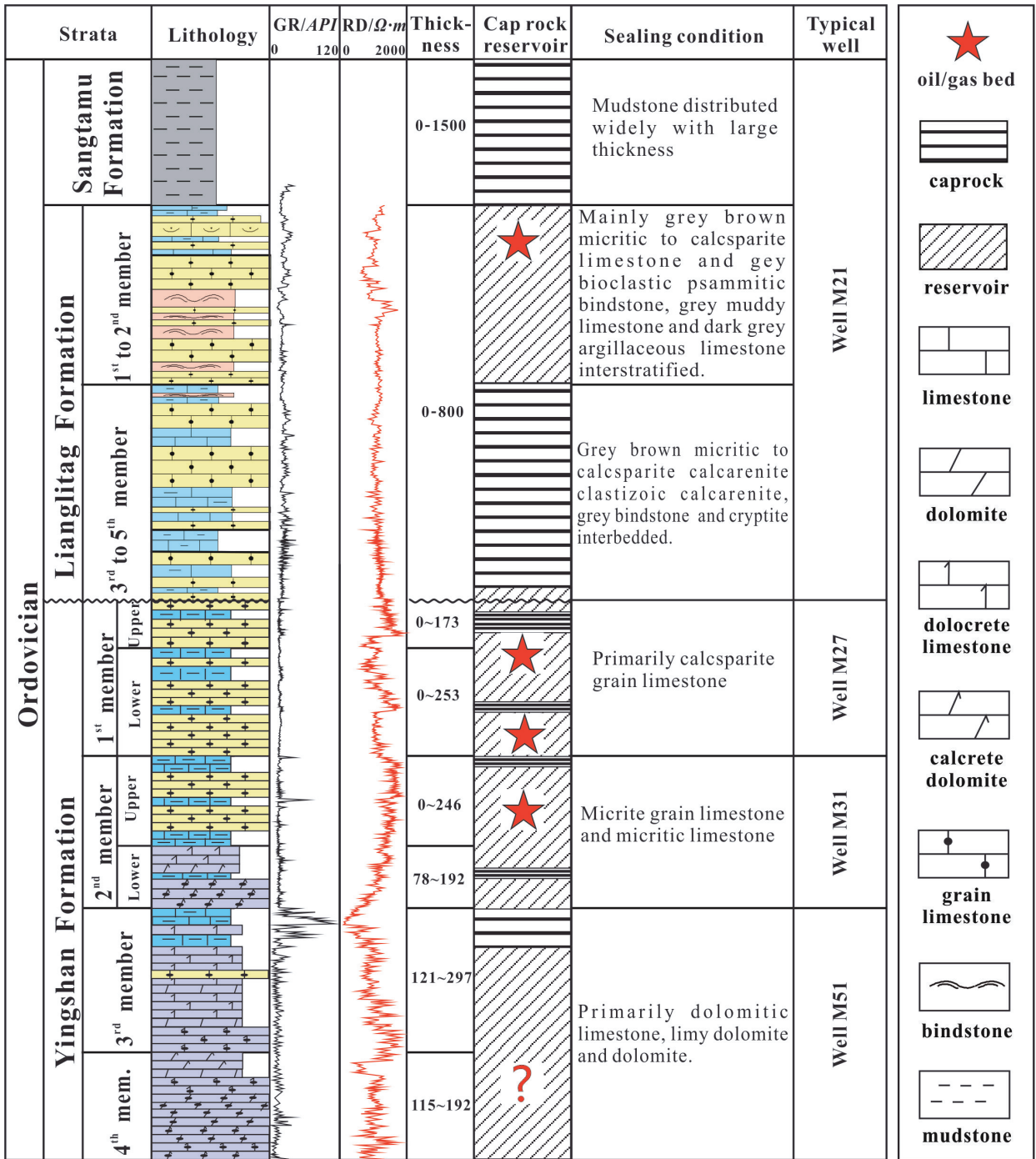


Figure 2. Generalized stratigraphy and lithology of Sangtamu Formation, Lianglitag Formation, and Yingshan Formation.

Fault Belt and this resulted in the disappearance of the 1st member and part of the upper section of the 2nd member near the Tazhong No. 10 Fault Belt. Therefore, high-resistivity layers Y1-G1 and Y1-G2 of the 1st member were preserved near the Tazhong No. 1 Fault Belt, but were denuded with the pinch-out of the 1st member toward the Central Fault Belt. High-resistivity layer Y1-

G1 is 0–65 m thick (65 m in well M17 and 50 m in well M14); layer Y1-G2 is 0–30 m thick (21 m in well M29 and 16 m in well M58). Of the 4 high resistivity layers in the 2nd member, layer Y2-G1 is 20–65 m thick (43 m in well M25); layer Y2-G2 is 10–30 m thick (18 m in well M61 and 23 m in well M19); layer Y2-G3 is 10–30 m thick (21 m in well M53); and layer Y2-G4, which is penetrated by

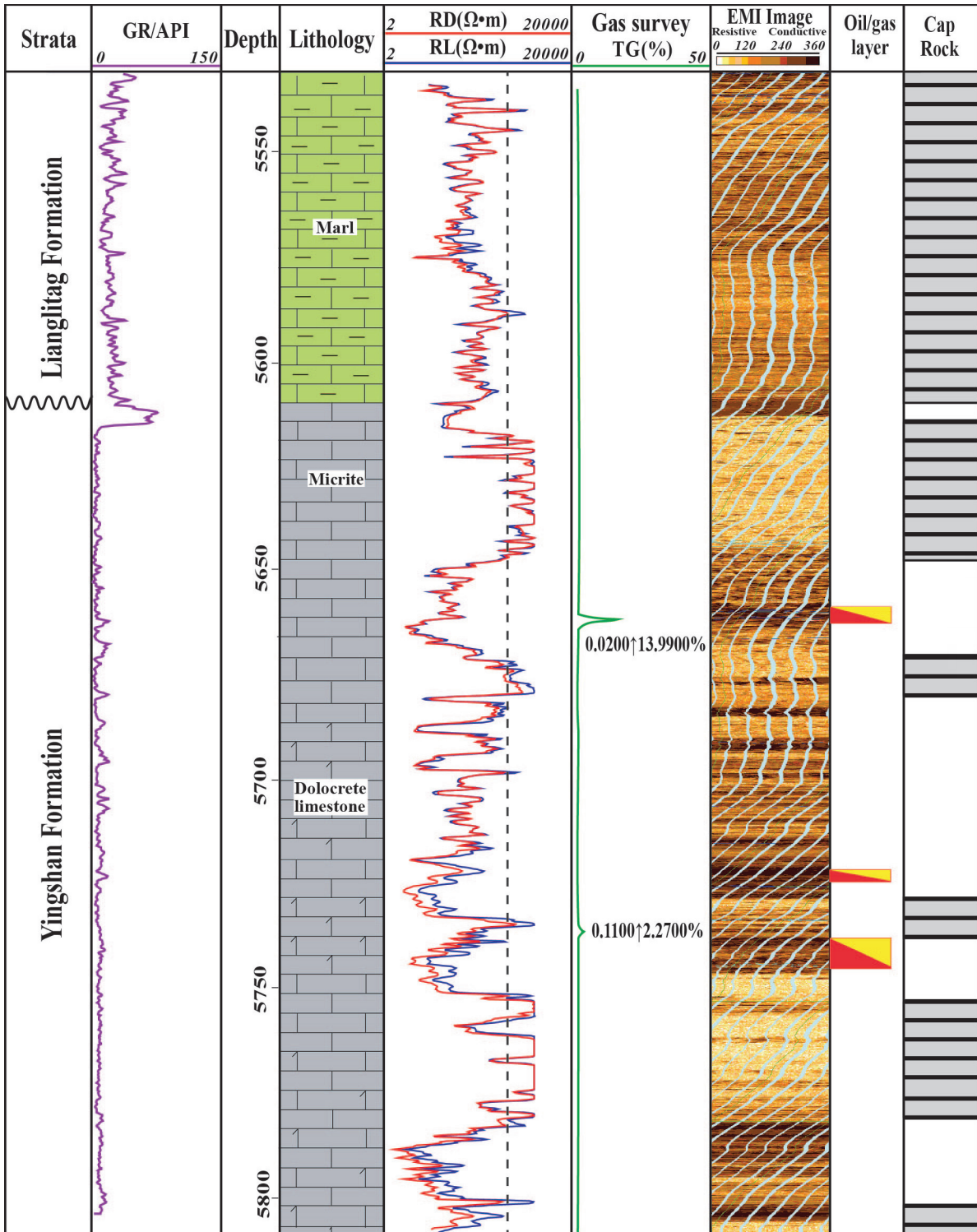


Figure 3. Characteristics of high-resistivity layers of Yingshan Formation in Well M20.

only a few wells, is 10–50 m thick (42 m in well M20). As mentioned previously, the high-resistivity layers and the reservoir beds constitute sequential seal–reservoir bed assemblages.

### 3.3. Sealing capability

The layers of oil and gas accumulations in the lower reservoir beds of the 1st and 2nd members of the Yingshan Formation (Figure 7) are all sealed by the 3rd to 5th



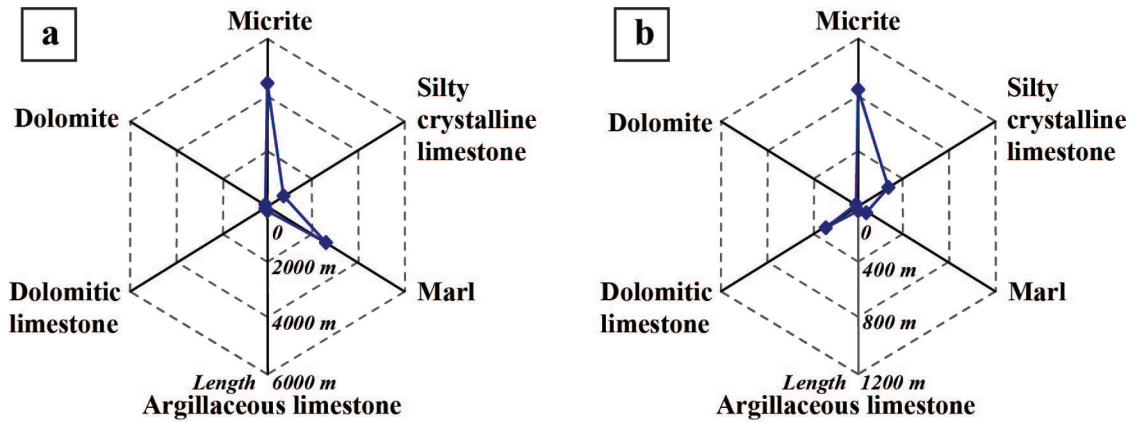


Figure 4. Lithologic characteristics of the carbonate cap rock in the Northern Slope of Tazhong Low Rise: a) 3rd to 5th Lianglitag members; b) high-resistivity layers of Yingshan Formation.

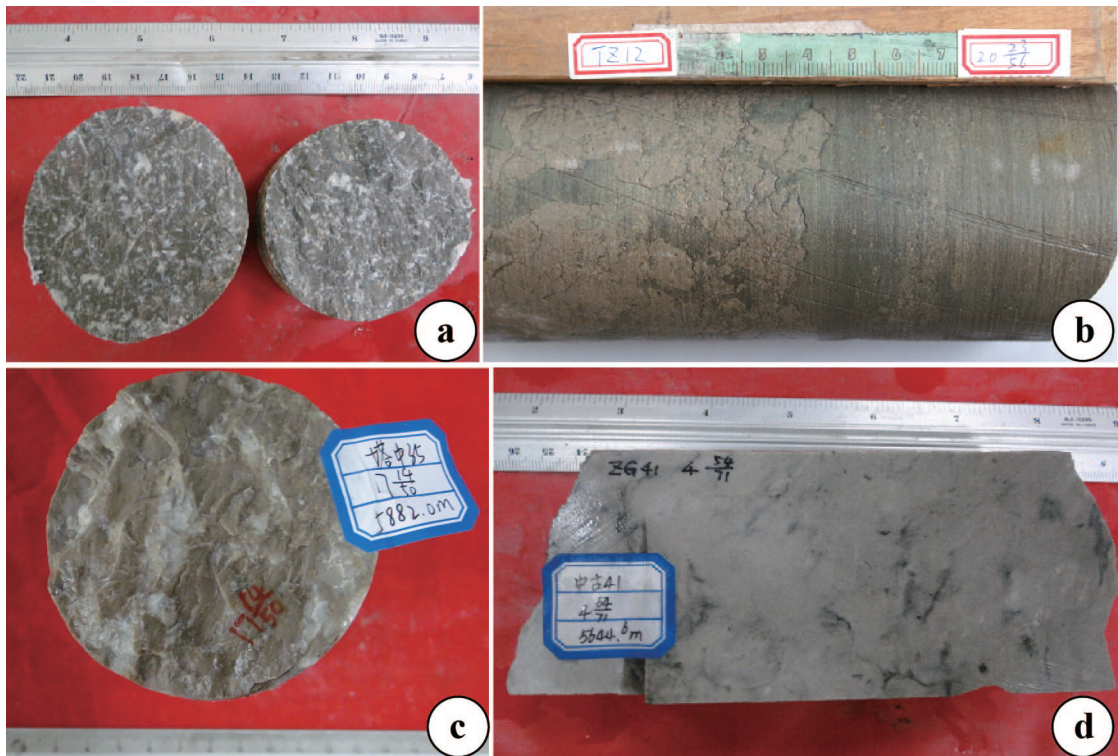


Figure 5. Characteristic core sample of the carbonate cap rock from on Northern Slope of Tazhong Low Rise: a) micrite, altered pores filled with calcite, well M35, 4983.4 m, O<sub>3</sub>I<sup>5</sup>; b) pelitic limestone, well M36, 4881.0 m, O<sub>3</sub>I<sup>3</sup>; c) micrite, altered pores filled with calcite, well M48, 5882.0 m, O<sub>1</sub>y; d) dolomite, well M49, 5644.6 m, O<sub>1</sub>y.

members of the Lianglitag Formation and the inner high-resistivity layers. The barrier layers not only seal oil and gas zones but also influence the movement of underlying fluid. Multiple volcanic hydrothermal activities took place on the Tazhong Northern Slope (Jia et al., 1995; Jin et al., 2006), and hydrothermal fluid was retained in place by barrier layers to reform and improve the Yingshan reservoir beds. For example, faults developed in the area

near well M35 in the east of the Tazhong Northern Slope, and hydrothermal fluid reformed the reservoir beds along the faults. Hydrothermal activity in the reservoir beds of the 1st and 2nd members of the Lianglitag Formation can be clearly tracked by means of various fingerprints, such as pyrite filling in the fractures in a core sample (Figure 8a). Similarly, the reformation of the 5th member of the Lianglitag Formation by hydrothermal fluid is detected



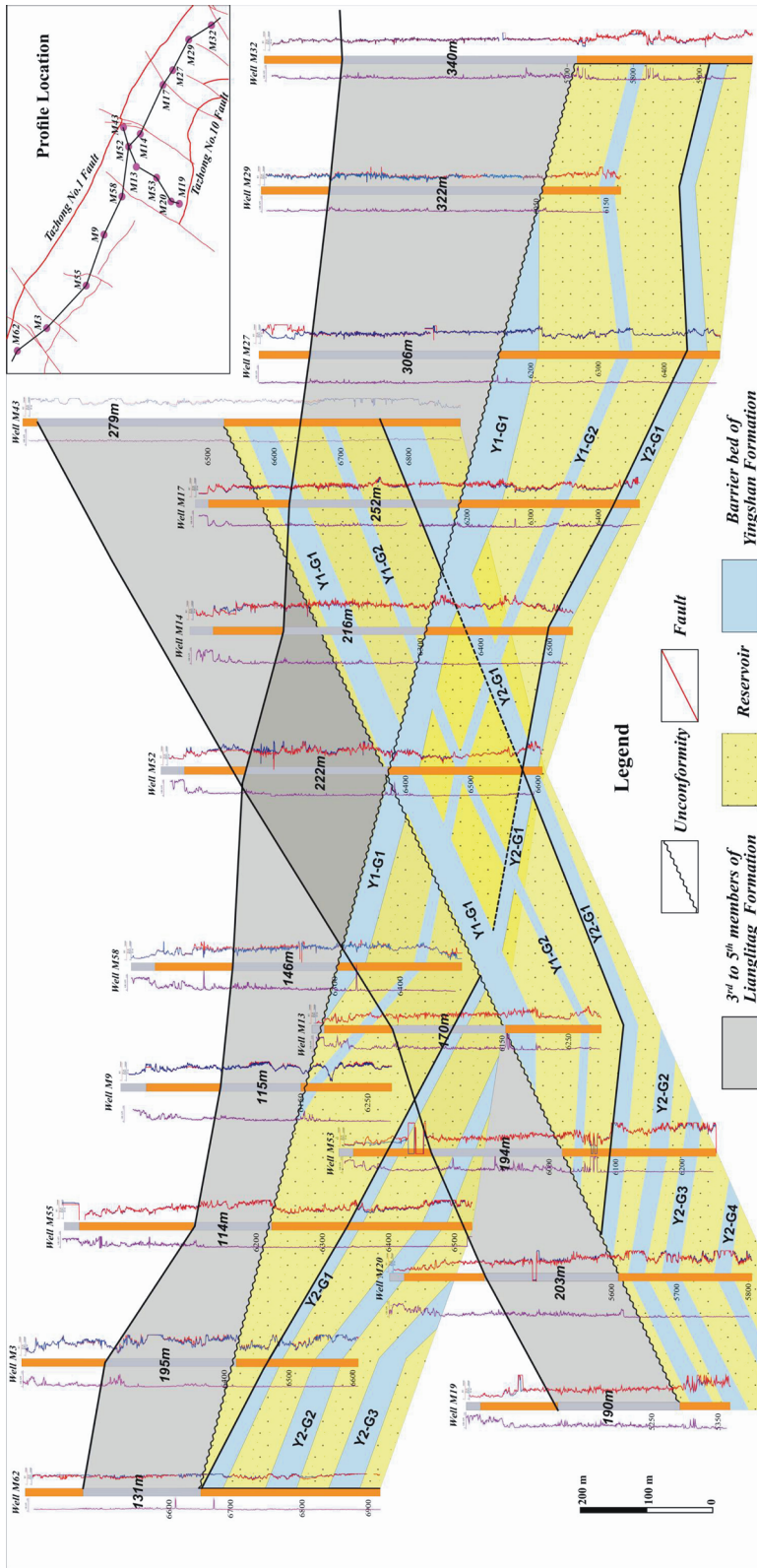


Figure 6. Fence diagram showing the distribution of cap rock on the Northern Slope of Tazhong Low Rise.

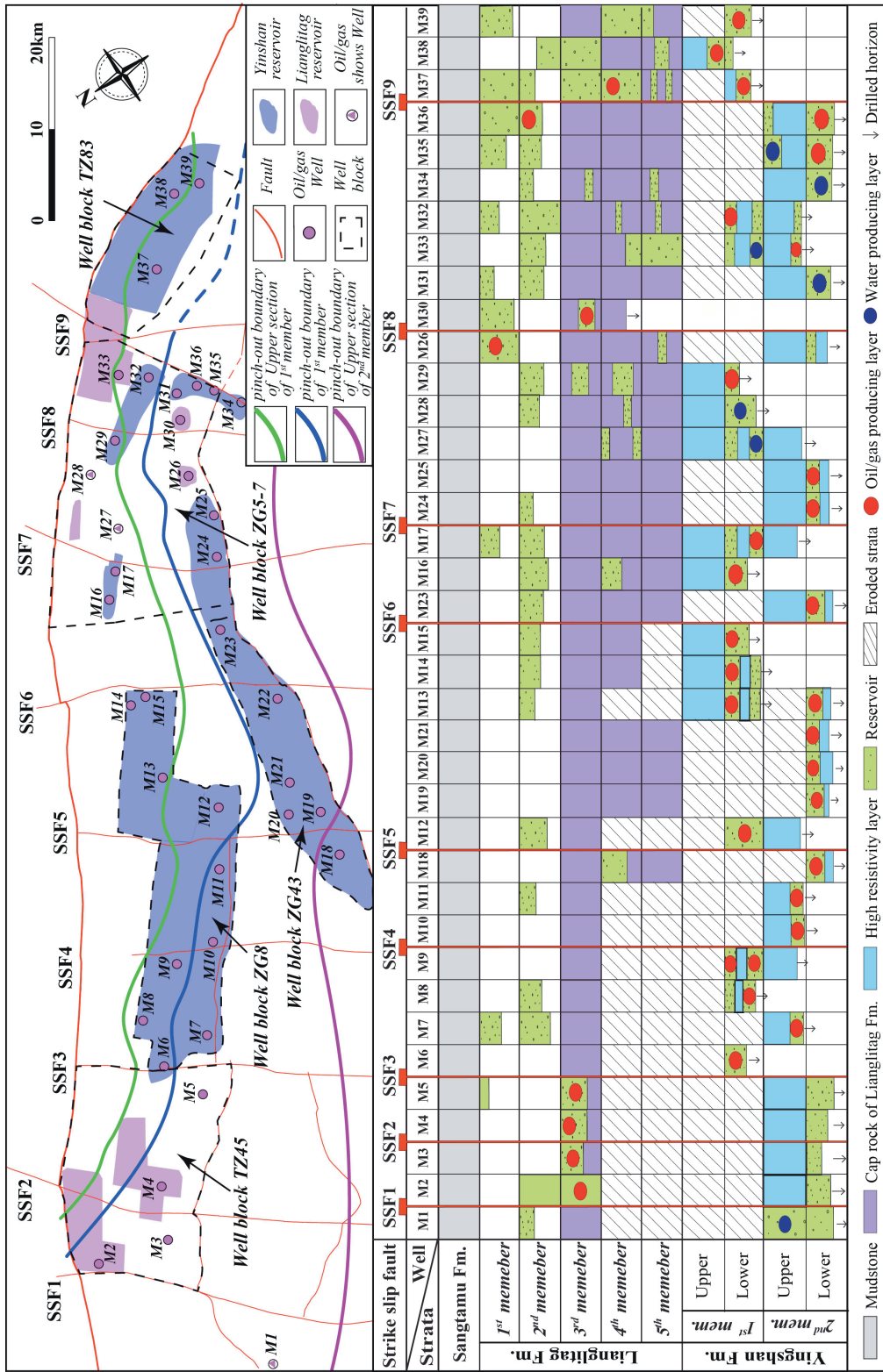
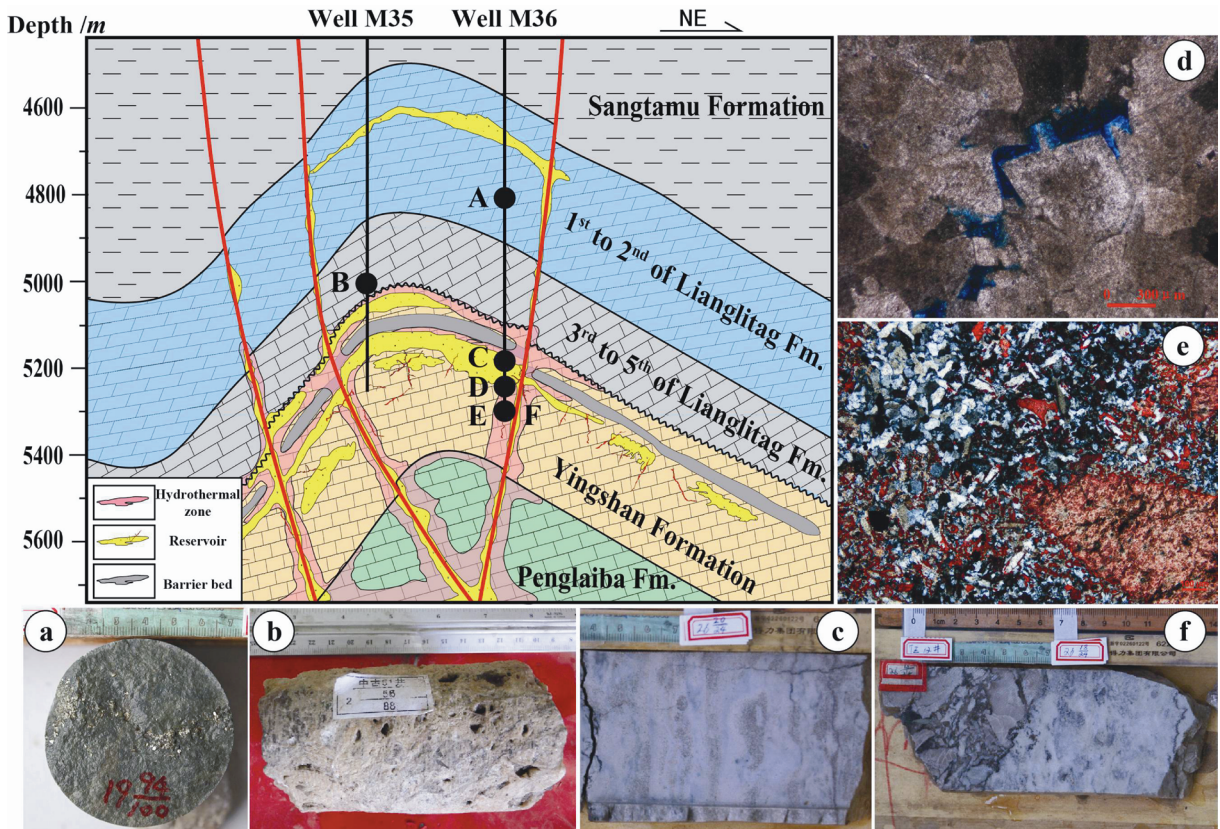


Figure 7. Distribution of cap rock on the Northern Slope of Tazhong Low Rise.





**Figure 8.** Model of reservoir bed reformation with hydrothermal fluid intrusion by carbonate cap rock: **a)** pyrite-filled fracture in a core of marl, from 4812-m depth in well M36; **b)** hydrothermal dissolution vugs in a core, from 5001-m depth in well M35; **c)** honeycomb pores in a core of hydrothermal dolomite with recrystallization, from 5225-m depth in well M36; **d)** crossed nicols microscope view of saddle dolomite, from 5234-m depth in well M36; **e)** crossed nicols microscope view of cherty limestone, from 5241-m depth in well M36; **f)** cherty limestone core piece, from 5241-m depth in well M36.

due to the formation of calcite recrystallization in the holes of a core sample recovered from this formation (Figure 8b). Coarse-grained dolomite and hydrothermal dolomite developed away from the faults to form honeycomb dolomite (Figures 8c and 8d). Medium- to fine-grained dolomite developed farther away from the faults. Silicification and hydrothermal metasomatism developed in the deeper reservoir beds near the faults (Figures 8e and 8f).

#### 4. Samples and method

The sealing capability of carbonate rock is difficult to evaluate with a single indicator or technique; the only way is to integrate the laboratory analysis, log-data analysis, and geological interpretation of sedimentary facies, stratigraphic correlation, diagenetic evolution, etc. The petrophysical properties of cap rock were investigated through the parameters of coreflood displacement pressure, permeability, porosity, density, and specific surface area and the analysis of micropore composition. The coreflood displacement pressure is the most direct

parameter indicating the sealing capability by actual measurement. In this study, 12 core samples from the 3rd to 5th members of the Lianglitag Formation, 9 core samples from the high-resistivity layers in the Yingshan Formation, and 5 core samples from the Yingshan reservoir beds were tested for displacement pressure. From each full-size core sample a core plug with the diameter of 2.5 cm was cut perpendicular to the bedding plane and was sequentially washed with a solvent, dried, desalinated by flooding or leaching, and dried. Each core plug was then saturated with a solution of aviation kerosene in a PH-2 type vacuum saturation apparatus for 4 days. The kerosene-saturated core plug was placed in the rubber sleeve of a core holder and circumferential liquid pressure was applied outside the rubber sleeve by means of a high-pressure pump so that the surface of the core plug was completely sealed by the rubber sleeve. Pure nitrogen gas was then injected into the core plug at a predetermined driving pressure. At the time ( $t_1$ ) of gas breakthrough at the outlet-end of the core plug, the injection pressure was recorded as the penetration pressure ( $P_1$ ). After saturating

the same core plug with the formation water, the injection procedure was repeated, at the end of which a new penetrating pressure ( $P_2$ ) and new breakthrough time ( $t_2$ ) were obtained. The Poiseuille equation, modified by the integral transformation (Huang and Hao, 1994) as in Eq. (1) below, was used to establish the relation between the penetrating pressure and breakthrough time. Eventually, Eq. (2) below was utilized to estimate the displacement pressure ( $P_0$ ). In order to ensure accuracy, the doubtful core samples were retested using the FYKS-2 type porosity and permeability tester, which was operated under high-temperature overburden pressure.

$$t = \frac{4L^2q^2\mu}{r_a(P_i - P_0)} \tag{1}$$

$$P_0 = \frac{P_2t_2 - P_1t_1}{t_2 - t_1} \tag{2}$$

Here,  $t$  is the breakthrough time,  $L$  is the sample length,  $q$  is the injection flow rate;  $\mu$  is the injection fluid viscosity,  $r_a$  is the correction parameter,  $P_i$  is the penetration pressure, and  $P_0$  is the displacement pressure.

Meanwhile, the cores, drill cuttings, and their thin-sections were examined under microscope, and statistical analysis was performed on the logging data, e.g., gamma ray (GR), porosity, fracture porosity, and electric resistivity.

## 5. Results and sealing evaluation

### 5.1. Sealing effectiveness

#### 5.1.1. Dense limestone in the 3rd to 5th members of the Lianglitag Formation

Sun et al. (2008) analyzed the relationship between cap rock thickness and the amount of reserves and found that 40 m is the minimum thickness for a gas reservoir with medium recovery efficiency and with the reserves of more than  $400 \times 10^6 \text{ m}^3/\text{km}$ ; 100 m is the minimum thickness for a gas reservoir with high recovery efficiency and with the reserves of more than  $1 \times 10^9 \text{ m}^3/\text{km}$ . The cap rock of the 3rd to 5th Lianglitag members is generally more than 80 m thick. From the relationship between thickness and the underlying oil and gas reserves it can be deduced that a cap rock thicker than 100 m can seal the oil and gas zones (Figure 9). For the seal thickness of more than 200 m, both the oil/gas recovery and gas/oil ratio (GOR) increase with increasing thickness, indicating an efficient sealing for gas.

The increase in shale content and decrease in porosity and permeability give the carbonate rock better sealing capability. The conventional GR log readings and the shale content also show a positive correlation. Statistical analysis of the log data in oil/gas wells has shown that the GR response of carbonate cap rock is less than 20 API in the pay zone in the Lianglitag reservoir bed, in the well

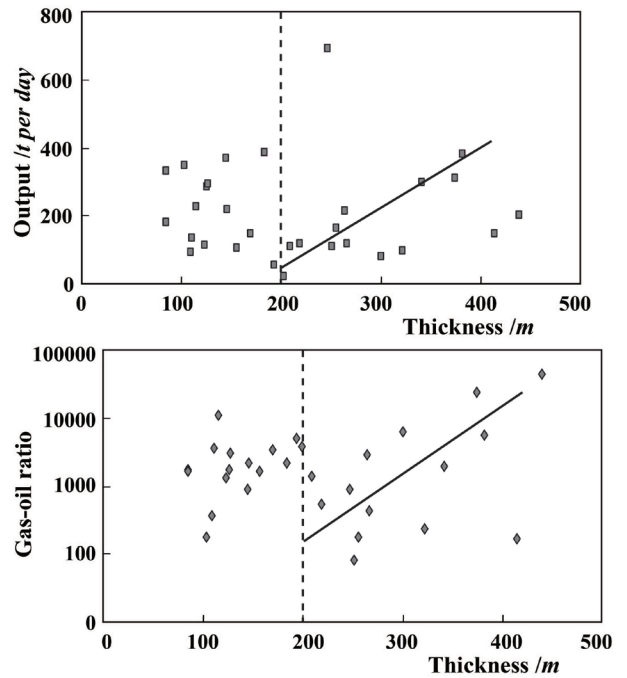


Figure 9. Variation of oil/gas output and gas-oil ratio with respect to the thickness of 3rd to 5th members of Lianglitag Formation.

blocks of M45 and M83 (Figure 10), and is more than 20 API in the pay zone in the Yingshan reservoir bed, in the well blocks of M8-43 and M5-7. Therefore, a GR response of 20 API is considered to be an important evaluation parameter for the sealing capability of the 3rd to 5th Lianglitag members.

In addition to shale content and porosity from log data, the sealing capability of carbonate was also evaluated by testing displacement pressure ( $P_d$ ) and calculated displacement pressure ( $P_c$ ). Generally, the higher the shale content and the lower the porosity were, the higher the displacement pressure was, which indicates good sealing

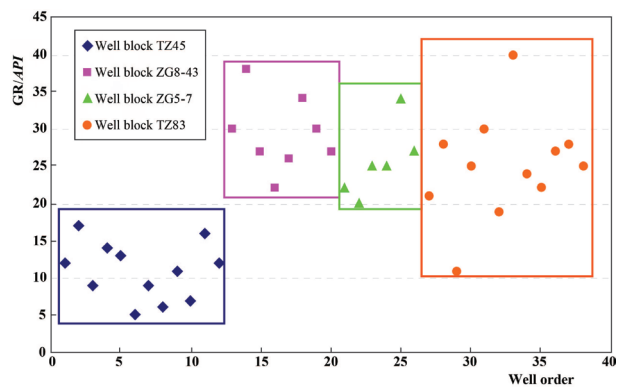


Figure 10. Gamma ray (GR) response of different oil- and/or gas-producing layers in various well blocks.

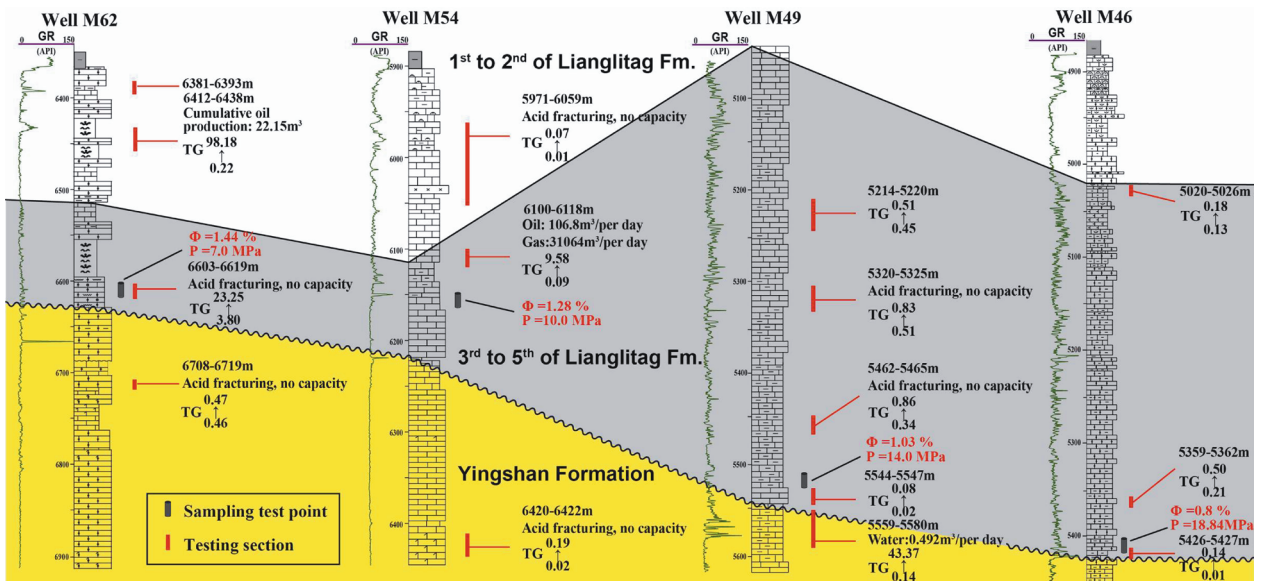


capability. Out of 13 core samples of the 3rd to 5th members tested, breakthrough was observed only in 3 samples at the pressure of 14 MPa (Table 1). Shale content (GR) and porosity ( $\Phi$ ) were correlated with the testing displacement pressures ( $P_d$ ) to obtain the calculated displacement pressure ( $P_c$ ). A comparison of the displacement pressures of core samples from 4 wells (Figure 11) showed that the sealing capability was poor for displacement pressures of less than 14 MPa, excluding faults' interference. For example, oil and gas seem to have migrated up through the cap rock ( $P_c < 14$  MPa) and were accumulated in the overlying 1st to 2nd Lianglitag members in the region of wells M62 and M54. On the other hand, the cap rock in the region of wells M49 and M46 seems to successfully prevent the oil/gas migration with  $P_c$  of more than 14 MPa. Therefore, the displacement pressure of 14 MPa is

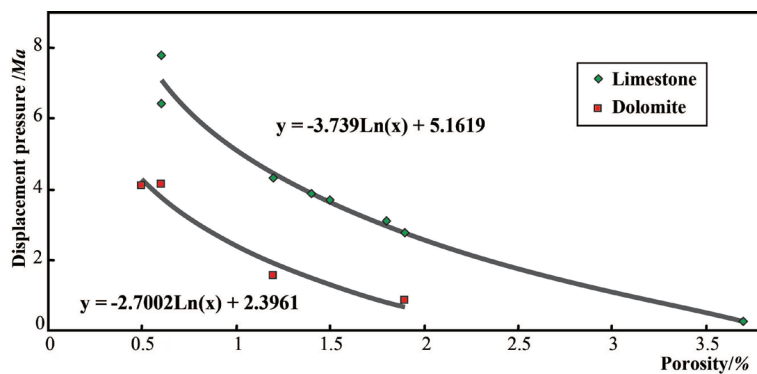
considered to be the lower limit for the sealing capability of carbonate cap rock in the 3rd to 5th Lianglitag members.

**5.1.2. High-resistivity layers in the Yingshan Formation**

Based on the test results obtained from 9 core plug samples of high-resistivity layers and from 5 core plug samples of the reservoir bed (Table 2), the displacement pressures of high-resistivity layers are found to be greater than 3 MPa and those of reservoir beds are found to be less than 3 MPa. Moreover, relatively high displacement pressures observed in the core samples of dolomitic limestone (4.70 MPa in sample M27-GY1 and 4.13 MPa in sample M47-GY1-2) are attributed to dolomitization and low intercrystal porosity. Note that the displacement pressures in dolomite samples were observed to be less than in limestone samples for the same porosity, as shown by 2 related curves in Figure 12.



**Figure 11.** The measured porosity and displacement pressure data (in red) for the core samples from 4 wells drilled through the effective sealing sections of the 3rd to 5th members of the Lianglitag Formation.



**Figure 12.** Variation of displacement pressure as a function of porosity in the high-resistivity layers of Yingshan Formation.

**Table 1.** Cap rock characteristics of the 3<sup>rd</sup> to 5<sup>th</sup> members of Lianglitag Formation.

No.	Sample	Depth (m)	Lithology	Thickness (m)	GR (API)	Fracture porosity (%)	Porosity ( $\Phi$ ) (%)	Displacement pressure ( $P_d$ ) (MPa)	Calculated displacement pressure ( $P_c$ ) (MPa)
1	M62-L	6601.70	Micrite	131	<u>14-24</u> 20.81	<u>0.003-0.007</u> 0.004	<u>1.2-1.9</u> 1.44	7.0	7.23
2	M54-L	6153.94	Micrite	104	<u>12-32</u> 22.00	<u>0.001-0.042</u> 0.017	<u>1.0-2.0</u> 1.28	10.0	9.65
3	M48-L	5775.36	Micrite	120	<u>27-46</u> 30	<u>0.031-0.152</u> 0.056	<u>0.6-1.5</u> 0.9	No breakthrough under 14 MPa pressure within 48 h	16.90
4	M12-L	5921.72	Argillaceous limestone	199	<u>24-34</u> 31.33	<u>0.003-0.019</u> 0.014	<u>0.1-0.6</u> 0.32	No breakthrough under 14 MPa pressure within 48 h	38.18
5	M36-L	4973.10	Argillaceous limestone	316	<u>17-20</u> 19.03	<u>0.01-0.015</u> 0.013	<u>0.3-1.4</u> 0.40	No breakthrough under 14 MPa pressure within 48 h	33.59
6	M46-L	5423.21	Micrite	400	<u>15-60</u> 25.00	<u>0.004-0.007</u> 0.005	<u>0.6-2.1</u> 0.8	No breakthrough under 14 MPa pressure within 48 h	19.32
7	M37-L	5468.14	Argillaceous limestone	352	<u>13-44</u> 22.14	<u>0.001-0.049</u> 0.002	<u>0.5-2.5</u> 0.58	No breakthrough under 14 MPa pressure within 48 h	25.94
8	M49-L	5542.20	Micrite	522	<u>10-40</u> 24.40	<u>0.001-0.03</u> 0.012	<u>0.5-2.5</u> 1.03	14.0	14.12
9	M51-L	4698.60	Micrite	504	<u>15-30</u> 20.05	<u>0.001-0.022</u> 0.008	<u>0.4-2.5</u> 0.76	No breakthrough under 14 MPa pressure within 48 h	20.38
10	M64-L	4647.40	Argillaceous limestone	884	<u>14-29</u> 23.06	<u>0.005-0.036</u> 0.027	<u>0.8-2.3</u> 0.89	No breakthrough under 14 MPa pressure within 48 h	17.13
11	M44-L	5808.41	Micrite	260 (not drilled through)	<u>3-20</u> 18.00	<u>0.001-0.059</u> 0.021	<u>0.1-1.9</u> 0.4	No breakthrough under 14 MPa pressure within 48 h	33.59
12	M45-L	5499.12	Micrite	182 (not drilled through)	<u>11-46</u> 21.00	<u>0.001-0.023</u> 0.003	<u>0.1-1.9</u> 0.6	No breakthrough under 14 MPa pressure within 48 h	25.24

$$P_c = -20.581 \times \ln(\Phi) + 14.731; \Phi = (2.71 - \text{DEN}) / (2.71 - 1.1).$$

**Table 2.** Cap rock characteristics of the high-resistivity layers of Yingshan Formation.

No.	Sample	Lithology	Depth (m)	Strata	Thickness (m)	Resistivity (LLD) ( $\Omega$ m)	Fracture porosity, $\phi_f$ (%)	Porosity, $\phi$	Casing press. (MPa)	Displacement pressure Pd (MPa)	Calculated pressure Pcl/Pcd (MPa)
1	M47-GY1-1	Micrite	4140.0	Y1-G1	13	1560	0.037	0.6	30	6.42	7.07
2	M32-GY1	Micrite	5838.8	Y1-G2	36.5	890	0.001	1.4	30	3.86	3.90
3	M47-GY1-2	Dolomitic limestone	4228.0	Y1-G2	8	3690	0.028	0.6	30	4.13	3.78
4	M27-GY1	Dolomitic limestone	6433.5	Y1-G2	21.5	1500	0.001	0.1	30	4.70	8.61
5	M41-GY2	Micrite	6498.0	Y2-G1	13 (not through)	1600	0.003	1.5	30	3.68	3.65
6	M49-GY2	Dolomitic limestone	5604.0	Y2-G2	30.5	12,000	0.005	0.5	30	4.08	4.27
7	M48-GY2	Micrite	5998.3	Y2-G4	20	10,000	0.007	0.6	30	7.78	7.07
8	M36-GY2	Micrite	5239.6	Y2-G4	25	3000	0.001	1.8	30	3.10	2.96
9	M36-GY2-2	Micrite	5250.5	Y2-G4	25	1000	0.09	1.2	30	4.32	4.48
10	M27-CY1	Micrite	6424.0	Reservoir	33	49	0.046	3.7	30	0.26	0.27
11	M27-CY2	Dolomitic limestone	6755.5	Reservoir	14	460	0.056	1.9	30	0.84	0.66
12	M49-CY2	Silty crystalline limestone	5600.0	Reservoir	7.5	54	0.012	3.4	30	0.61	0.59
13	M36-CY2-1	Dolomite	5244.5	Reservoir	6	300	0.1	1.2	30	1.56	1.90
14	M48-CY2	Micrite	5880.7	Reservoir	11	700	0.041	1.9	30	2.75	2.76

$\Phi_f = (1 / \text{LLD}^2 - 1 / \text{LLS}^2) \times R_{mf} \times \text{LLD} \times 100$  (LLD < LLS);  $\Phi_f = (1 / \text{LLS}^2 - 1 / \text{LLD}^2) \times R_{mf} \times \text{LLD} \times 200$  (LLD > LLS);  $R_{mf} = 0.128 \Omega \cdot \text{m} / 139.09^\circ \text{C}$ ;  $\Phi = (2.71 - \text{DEN}) / (2.71 - 1.1)$ .  
 $P_{cd} = -3.739 \times \text{Ln}(\Phi) + 5.1619$ ;  $P_{cd} = -2.7002 \times \text{Ln}(\Phi) + 2.3961$ ;  $P_{cd}$  = calculated pressure of limestone;  $P_{cd}$  = calculated pressure of dolomite (or dolomitic limestone).

The regression equations for these 2 curves were used to calculate the displacement pressures in the formations of pertinent lithology and for the prevailing level of porosity. Despite the displacement pressures in the samples of high-resistivity inner layers of the Yingshan Formation being lower than those of the samples of the 3rd to 5th members of the Lianglitag Formation, the exploration of the Tazhong Northern Slope has proven the isolated vertical zonation of the hydrocarbon accumulation in the Yingshan reservoir beds (Figures 7 and 13). For example, evidence for efficient sealing capability of high-resistivity layers is encountered in wells M20 and M63.

Although the porosity difference between the high-resistivity layers and their underlying reservoir beds varies widely, the displacement pressure differential between them is high in general. A high-resistivity layer can provide a seal for the underlying oil and gas zone, provided that the pressure difference is at or above the critical value of 6 MPa. When the pressure difference is less than 6 MPa, oil and gas shows are found in the overlying reservoir beds (Table 3) and the underlying reservoir bed may produce oil, gas, water, or nothing, which is the indication of poor sealing capability of such high-resistivity layers, as observed in wells M32, M9, and M59. If the pressure differential is greater than 6 MPa, oil/gas/water or nothing may be found in the overlying reservoir bed, but the underlying reservoir bed will produce oil and/or gas, which indicates the good sealing capability of such high-resistivity layers. For instance, in well M35, as the overlying reservoir bed produces water the underlying reservoir bed produces oil and gas, indicating the good sealing capability of the high-resistivity layer (Table 3). Consequently, the difference of 6 MPa is considered to be the lower limit of sealing capability of high-resistivity layers.

## 5.2. Controlling factors of carbonate cap rock

### 5.2.1. Sedimentation

The original sedimentary facies directly influenced the distribution and the sealing capability of the cap rock. According to Yuan et al. (2012), the sedimentary facies of the Yingshan Formation are of the slope-edge platform and open platform. The major sedimentary facies of high-resistivity layers were deposited in the interbank seas and low-lying platforms with deep seawater and low depositional energy, which resulted in the development of micrite, silty crystalline limestone, and biomicrite with medium to large bed thickness.

During the sedimentation of the 3rd to 5th members of Lianglitag Formation, the reef flat became smaller and the interbank sea deposition of mainly argillaceous limestone with substantial thickness occurred in between the platform margin reefs. The lithology of these sediments then controlled the sealing capability of the cap rock. In general, primarily the argillaceous limestone (in samples

M12-L and M36-L) and secondarily the micrite (in samples M62-L and M54-L) exhibit strong sealing capability. However, the dolomitic limestone and dolomite (in sample M36-CY2-1) have weak sealing capability. For the same porosity, the sealing capability of dolomitic limestone (in sample M47-GY1-2) is less than that of micrite (in sample M47-GY1-1). The difference in displacement pressure and porosity relationship for limestone and dolomite (Figure 12) may be attributed to mineral matrix porosity. For the carbonate cap rock, the greater the thickness is, the more difficult is the fracturing-induced destruction of the sealing capability that is stronger due to the hydrocarbon saturation and limited capillarity.

### 5.2.2. Diagenesis

Analyses conducted on the core samples have revealed that the carbonate rock experienced complex porosity changes during late diagenesis. Primary pores were formed in the deposition phase, and secondary pores were formed in the early diagenesis (exposure) phase. Most of the pores were partially preserved through the changes in the late diagenesis phase and, hence, a good reservoir bed was formed by the carbonate rock, which otherwise would have become a cap rock upon the destruction and vanishing of those pores. In particular, the late filling and cementation by calcite, recrystallized dolomite, and silicification during diagenesis significantly influenced the development of sealing capability of the cap rock. The observations and analyses conducted on 31 thin sections of high-resistivity layers revealed (Table 4; Figure 14) that the cement content was generally more than 10% and up to 31%, while the cement content in the reservoir bed was generally less than 10%. SEM images of the rock specimens from the 3rd to 5th members of the Lianglitag Formation, which is relatively dense with high cement content, show that an intergranular pore of calcarenite was filled with coarse-grained calcite (Figure 15a) and an intergranular hole was only 1 to 2  $\mu\text{m}$  in diameter due to the presence of illite or other clay minerals (Figures 15a and 15b). Calcite was the main cement that filled the intergranular pores, early pores, fractures, and crevices. The thin-section analyses conducted using polarized light and cathode-ray luminescence provided the detection of 2 phases of cement formation in a sample (Figures 16a and 16b) and even 4 phases of cement formation in another sample (Figures 16c and 16d). Both phases of cement formation occurred through the complex and everlasting diagenesis during the long process of deep burial. However, early microcrystalline cement residues are still observed in individual samples (Figure 16, marked I). Calcite cement seems to help the improvement of sealing capability, just as a limy mudstone (mudstone with an adequate amount of carbonate cements) does in the Tu-ha Basin or a mudstone with some dolomite (10%–15%) does in the Liaohe Basin,



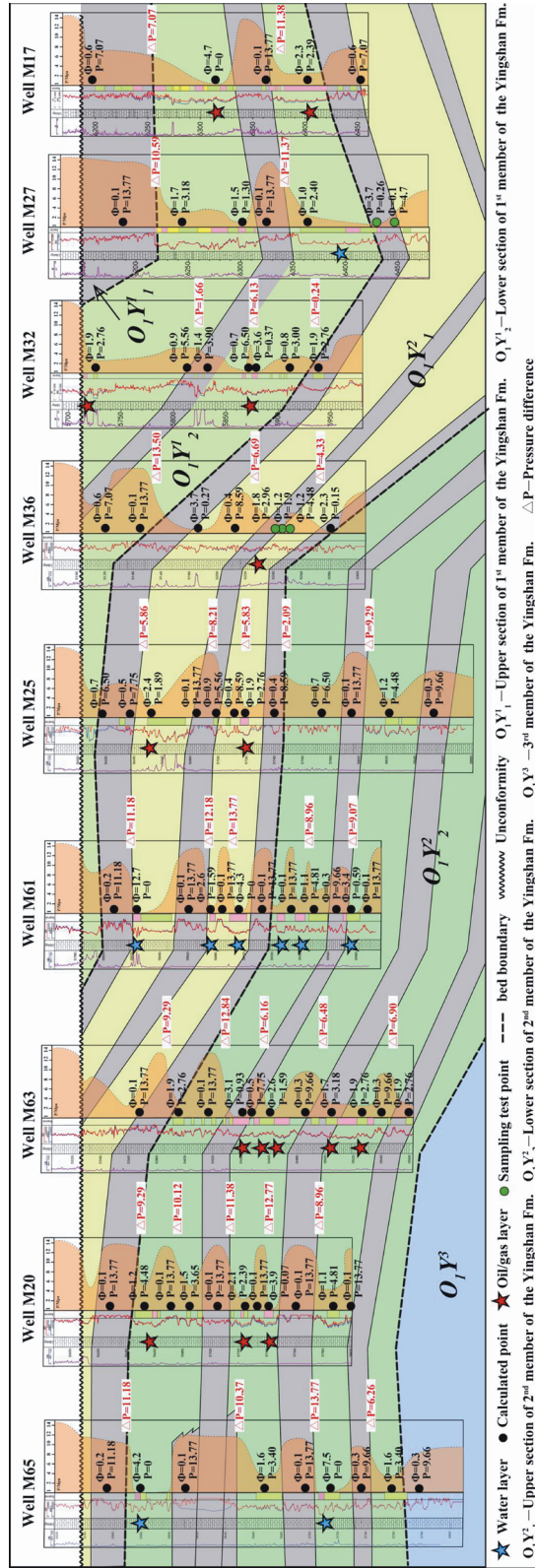
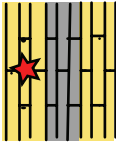
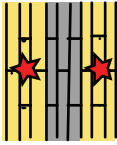
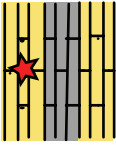

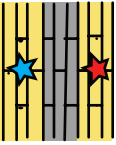
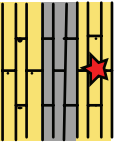


Figure 13. Comparison of displacement pressures in the vertical zonation of the high-resistivity layers and the oil/gas- or water-saturated beds in Yingshan Formation.

**Table 3.** The relationship between the pressure difference and effective sealing of high-resistivity layers.

Well	Depth (m)	High-resistivity layer			Underlying reservoir			Pressure difference (MPa)	Cap rock sealing
		Lithology	Porosity (%)	Calculated displacement pressure (MPa)	Lithology	Porosity (%)	Calculated displacement pressure (MPa)		
M32	5923	Micrite	0.8	6.00	Silty crystalline limestone	1.9	2.76	3.24	
M36	6165	Micrite	1.4	3.90	Intrasparite	6.89	0.00	3.90	
M59	6180	Silty crystalline limestone	0.58	7.20	Silty crystalline limestone	2.4	1.89	5.31	
M59	6110	Silty crystalline limestone	0.7	6.50	Silty crystalline limestone	3.13	0.90	5.60	
M35	5122	Micrite	0.7	6.50	Dolomitic limestone2..0		0.51	5.98	
M26	5551	Micrite	0.21	11.00	Intrasparite	1.1	4.84	6.16	

The red star represents the oil- and gas-producing pay, while blue represents the water-bearing layer.

**Table 4.** The results of thin-section analysis of high-resistivity layers and reservoir rock.

Well	Lithology	Strata	Depth (m)	DDL ( $\Omega$ m)	Percentage composition (%)					Reservoir/cap rock
					Calcite	Dolomite	Grain	Mud	Cement	
M50	Dolomitic limestone	O <sub>1</sub> y	3723.8	3603	85	15	59	10	31	Cap rock
	Dolomite	O <sub>1</sub> y	3761.6	655	20	80	77	13	10	Reservoir
	Dolomitic limestone	O <sub>1</sub> y	3834.2	2700	88	12	79	4	17	Cap rock
	Dolomitic limestone	O <sub>1</sub> y	3894.3	6082	71	29	62	15	23	Cap rock
	Limy dolomite	O <sub>1</sub> y	3959.1	1524	26	74	78	11	11	Cap rock
	Dolomite	O <sub>1</sub> y	4021.7	1006	8	92	88	2	10	Cap rock
M37	Dolomitic limestone	O <sub>1</sub> y	4022.3	898.8	85	15	70	13	17	Cap rock
	Dolomitic limestone	O <sub>1</sub> y	5624.2	170	86	14	91	1	8	Reservoir
	Dolomitic limestone	O <sub>1</sub> y	5683.2	180	84	16	74	10	16	Reservoir
M47	Dolomitic limestone	O <sub>1</sub> y	4148.0	830	86	14	77	19	4	Reservoir
	Dolomitic limestone	O <sub>1</sub> y	4152.7	830	87	13	88	4	8	Reservoir
M36	Limy dolomite	O <sub>1</sub> y	4157.1	830	28	72	93	2	5	Reservoir
	Dolomite	O <sub>1</sub> y	5231.8	300	5	95	98	1	1	Reservoir
	Dolomite	O <sub>1</sub> y	5241.6	3000	11	89	88	2	10	Cap rock
M32	Dolomitic limestone	O <sub>1</sub> y	5243.6	300	90	10	90	3	7	Reservoir
	Dolomitic limestone	O <sub>1</sub> y	5834.9	890	83	17	74	16	10	Reservoir
M49	Dolomitic limestone	O <sub>1</sub> y	5839.7	890	84	16	87	8	5	Reservoir
	Dolomitic limestone	O <sub>1</sub> y	5562.1	6000	86	14	81	9	10	Cap rock
M34	Dolomitic limestone	O <sub>1</sub> y	5602.7	12000	87	13	60	25	15	Cap rock
	Dolomitic limestone	O <sub>1</sub> y	5547.6	1300	86	14	70	3	27	Cap rock
M41	Dolomitic limestone	O <sub>1</sub> y	5586.4	390	79	21	89	3	8	Reservoir
	Dolomitic limestone	O <sub>1</sub> y	5595.5	130	86	14	87	3	10	Reservoir
	Dolomitic limestone	O <sub>1</sub> y	6492.1	1600	85	15	88	2	10	Cap rock
M57	Dolomitic limestone	O <sub>1</sub> y	6496.2	1600	88	12	75	11	14	Cap rock
	Limy dolomite	O <sub>1</sub> y	5572.2	1700	23	77	88	2	10	Cap rock
	Limy dolomite	O <sub>1</sub> y	5578.5	1090	35	65	88	1	11	Cap rock
	Dolomite	O <sub>1</sub> y	5580.8	519	4	96	97	1	2	Reservoir
M43	Limy dolomite	O <sub>1</sub> y	5594.4	908	31	69	90	7	3	Reservoir
	Limy dolomite	O <sub>1</sub> y	5617.7	991	31	69	90	2	8	Reservoir
M56	Dolomitic limestone	O <sub>1</sub> y	6755.4	688	85	15	45	51	4	Reservoir
M56	Dolomitic limestone	O <sub>1</sub> y	6595.9	2000	57	43	83	2	15	Cap rock

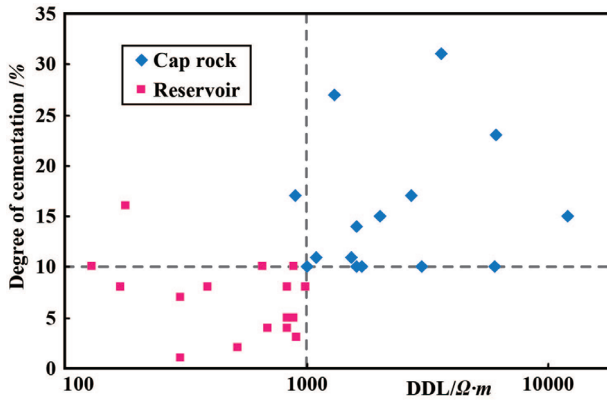


Figure 14. Comparison of cement content with respect to deep resistivity response in reservoir beds and cap rock.

where the breakthrough pressure is higher than the pure mudstone at the same depth (Huang and Deng, 1995).

### 5.2.3. Tectonism

Ordovician carbonate rock, which has well-developed fractures and crevices as the result of carbonate dissolution, has experienced multiple tectonic movements. Carbonate rock near faults was easily broken due to the significant variation of some of its physical properties, e.g., porosity and permeability, and its sealing capability became weaker or even disappeared with unstable lateral variation. The tectonic movements caused the Tazhong Northern Slope to be cut by several NE strike-slip faults (Figures 1 and 7). The faults that cross the relatively thin 3rd to 5th members of the Lianglitag Formation are detected in wells M55 and M26 in the west, where the 4th to 5th members disappear. In addition to the aforementioned faults, the well-developed faults and fractures that cross the thick 3rd to 5th members of the

Lianglitag Formation in the east established the migration paths for oil and gas, which migrated upward through these paths and accumulated in the 1st and 2nd members of the Lianglitag Formation. The occurrence of such a fault and fracture system caused the reformation of some parts of the 3rd member from the nonreservoir bed to an oil and gas accumulation medium, which is encountered in well M30.

## 6. Conclusions

1) The lithology of Lianglitag carbonate cap rock and Yingshan inner barrier layers is primarily micrite on the Tazhong Northern Slope. The 3rd to 5th members of the Lianglitag Formation are highly shaly, and barrier layers in the Yingshan Formation are more dolomitic. The cement content of the barrier layers is generally more than 10% and that of the reservoir bed is generally less than 10%. The 3rd to 5th members of the Lianglitag Formation are relatively dense with high cement content, which is observed in thin-section analysis as an intergranular pore of calcarenite being filled with coarse calcite cement and as the reduction of throat size of an intergranular pore to 1 to 2  $\mu\text{m}$  due to being filled with clay.

2) The cap rock of the 3rd to 5th Lianglitag members is more than 100 m thick and can seal oil and gas zones. The oil/gas recovery and GOR increase with increasing thickness beyond 200 m, indicating a good sealing for gas. Argillaceous limestone has better sealing capability for oil and gas than micrite. Generally, the 3rd to 5th members, with GR response greater than 20 API and displacement pressure greater than 14 MPa, serve as good direct cap rock that provides efficient sealing for oil and gas zones.

3) Six stable inner barrier layers with the thickness of several tens of meters are present in the 1st and 2nd members of the Yingshan Formation. Displacement

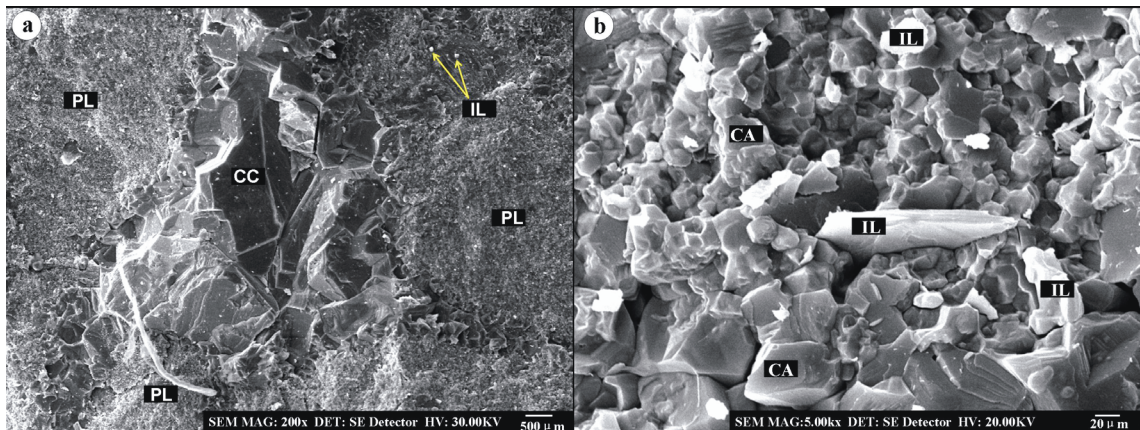
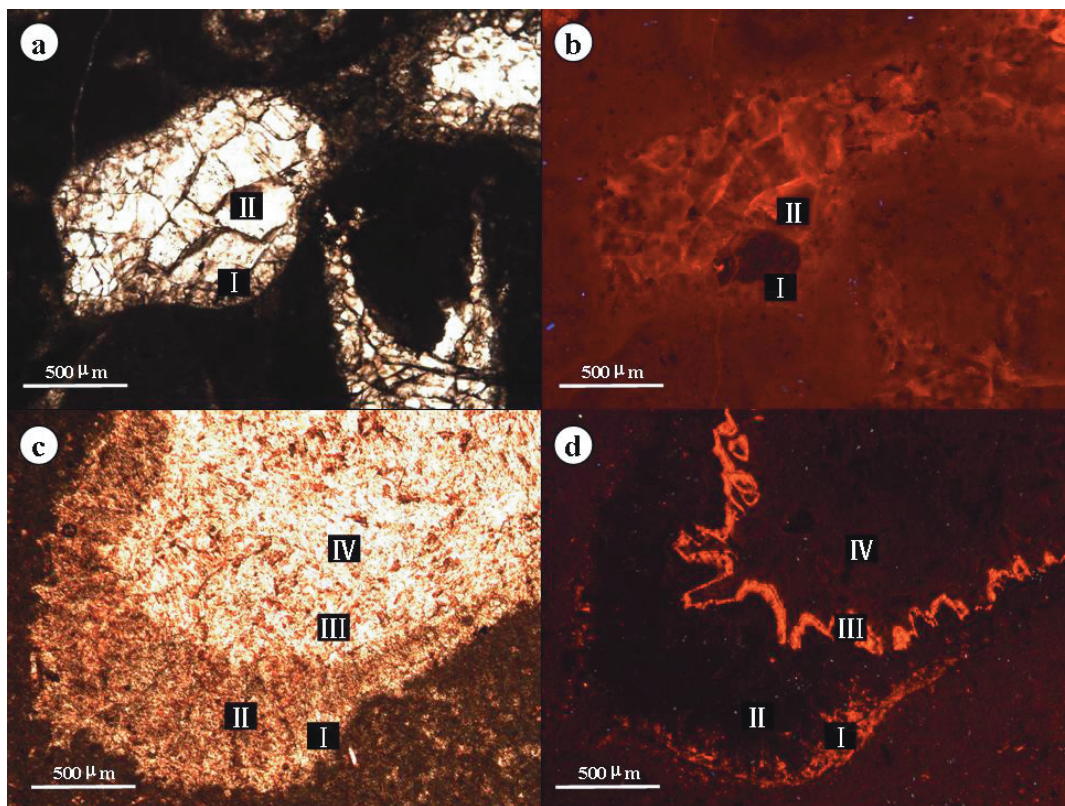


Figure 15. Scanning electron microscope images of carbonate cap rock of 3rd and 5th members of Lianglitag Formation: a) gray grain limestone, intergranular fracture filled with coarse calcite, intercrystalline pore filled with illite flake, well M83, O<sub>3</sub>1, 5334.5 m; b) gray bioclastic limestone, intercrystalline pore spaces of 1–2  $\mu\text{m}$  with illite flakes, well M83, O<sub>3</sub>1, 5446.7 m; CC- coarse calcite; IL- illite; PL- psammitic particle; CA- calcite.





**Figure 16.** Different periods of intergranular calcite cement: **a, b** micrite with 2 phases of calcite cement marked I and II, from 5073 m of depth in well M36; **c, d** micrite with 4 phases of calcite cement marked I to IV, from 6401 m of depth in well M40. (a) and (c) are under plane polarized light and (b) and (d) are under cathode-ray luminescence.

pressure in dolomite is lower than that of limestone for the same porosity. Barrier layers with displacement pressure 6 MPa higher than that of the underlying reservoir bed could provide good sealing.

4) Carbonate cap rock is controlled by the original sedimentary facies and is influenced by the late diagenesis to become dense with high cement content. Generally, a relatively stable lateral distribution is exhibited by the direct cap rock and the inner barrier layers, and the latter form several sequential sets of a reservoir bed-sealing layer assemblage, which cause the vertical zonation of hydrocarbon accumulations that are clearly identified in the Yingshan Formation. In the case of sealing failure of the direct cap rock, oil and gas could migrate further upwards through the fault system and

accumulate in overlying 1st and 2nd members of the Lianglitag Formation, which is sealed by the regional cap rock of Sangtamu mudstone.

#### Acknowledgments

The authors thank the researchers at the Tarim Oilfield Company of PetroChina for their helpful discussions and suggestions. They also thank the referees and editors for carefully reviewing and improving earlier versions of the manuscript significantly. This work was supported by the State Key Program of National Natural Science of China (Grant No. 41130422), the Major National S&T Program (Grant No. 2011CB201100-03), and the CUP Doctorial Basic Innovation Research Fund (Grant No. 2462013YXBS002).

#### References

- Alekseev AS, Kononova LI, Nikishin AM (1996). The Devonian and Carboniferous of the Moscow Syncline (Russian Platform): stratigraphy and sea-level changes. *Tectonophysics* 268: 149–168.
- Alsharhan AS, Nairn AEM (1997). *Sedimentary Basins and Petroleum Geology of the Middle East*. Amsterdam, the Netherlands: Elsevier.
- Bai GP (2007). A preliminary study of main control factors on oil and gas distribution in Persian Gulf Basin. *J China Univ Petrol* 31: 28–32 (in Chinese).
- Beydoun ZR (1988). *The Middle East: Regional Geology and Petroleum Resources*. Beaconsfield, UK: Scientific Press.

- Cheng QQ, Chen HY, Fan M, Wang Q, Chen WJ (2006). Determination of the total pore texture of cap rock. *Petrol Geol Exp* 28: 604–606 (in Chinese).
- Fan JF (2009). Prediction of exploration potential area of Leikoupo formation in Western Sichuan Depression. *Geophys Prospect Petrol* 48: 417–424 (in Chinese).
- Fan M, Chen HY, Yu LJ, Zhang WT, Liu WX, Bao YJ (2011). Evaluation standard of mudstone caprock combining specific surface area and breakthrough pressure. *Petrol Geol Exp* 33: 87–90 (in Chinese).
- Fu G, Hu M, Yu D (2010). Volcanic cap rock type and evaluation of sealing gas ability: an example of Xujiaweizi Depression. *J Jilin Univ* 40: 237–244 (in Chinese).
- Grunau HR (1987). A worldwide look at the cap rock problem. *J Petrol Geol* 10: 245–266.
- Han JF, Yu HF, Zhang HZ, Luo CS, Jing B, Huang GJ, Ji YG, Dong RX (2008). Characteristics of hydrocarbon enrichment in the Lower Ordovician carbonate rock weathering crust on the northern slope zone of Tazhong area. *Oil Gas Geol* 29: 167–188 (in Chinese).
- Huang HP, Deng HW (1995). The mudstone sealing and its impact factors. *Nat Gas Geosci* 6: 20–26 (in Chinese).
- Huang ZL, Hao SS (1994). A method of estimating breakthrough pressure and displacement pressure of cap rock. *Xinjiang Petrol Geol* 15: 163–166 (in Chinese).
- Jia CZ, Wei GQ, Yao HJ (1995). Tectonic Evolution and Regional Structural Geology. Beijing, China: Petroleum Industry Press (in Chinese).
- Jiao CH, Gu YF (2004). Application of log data in evaluating Caprocks. *Well Logging Technol* 28: 45–47 (in Chinese).
- Jin ZJ, Zhu DY, Hu WX, Zhang XF, Wang Y, Yan XB (2006). Geological and geochemical signatures of hydrothermal activity and their influence on carbonate reservoir beds in the Tarim Basin. *Acta Geol Sin* 80: 245–253 (in Chinese).
- Kashfi MS (1992). Geology of the Permian “super-giant” gas reservoirs in the greater Persian Gulf area. *J Petrol Geol* 15: 465–480.
- Klemme HD (1975). Giant oil fields related to their geologic setting: a possible guide to exploration. *B Can Petrol Geol* 23: 30–66.
- Klemme HD (1980). Petroleum basins-classifications and characteristics. *J Petrol Geol* 3: 187–207.
- Li B, Zhu XM (2012). Petroleum geology and exploration potential of Volga-Ural Basin: one typical foreland basin. *Petrol Geol Exp* 34: 47–52 (in Chinese).
- Li BL, Guan SW, Li CX, Wu GH, Yang HJ, Han JF, Luo CS, Miao JJ (2009). Paleo-tectonic evolution and deformation features of the Lower Uplift in the Central Tarim Basin. *Geol Rev* 55: 521–520 (in Chinese).
- Li GP, Zheng DW, Ouyang YL (1996). Sealing Capacity and Evolution of Cap Rock for Gas. Beijing, China: Petroleum Industry Press (in Chinese).
- Lin CS, Yang HJ, Liu JY, Rui ZF, Cai ZZ, Li ST, Yu BS (2012). Sequence architecture and depositional evolution of the Ordovician carbonate platform margins in the Tarim Basin and its response to tectonism and sea-level change. *Basin Res* 24: 559–582.
- Lu XS, Jiang YL, Song Y (2007). Influence of mechanical properties and stress state of caprock on its sealing performance: taking Kela-2 gas field as an example. *Nat Gas Ind* 27: 48–51 (in Chinese).
- Lü Y, Zhang SC, Wang YM (2000). Research of quantitative relations between sealing ability and thickness of cap rock. *Acta Petrolei Sin* 21: 27–30 (in Chinese).
- Lü YF, Fu G (1996). The Sealing of Oil/Gas Reservoir. Beijing, China: Petroleum Industry Press (in Chinese).
- Macgregor DS (1986). The hydrocarbon systems of North Africa. *Mar Petrol Geol* 13: 329–340.
- Mei MX, Zhang H, Meng XQ, Chen YH (2006). Sequence stratigraphic division and framework of the Lower Cambrian in the Upper Yangtze region. *Geol China* 33: 1292–1304 (in Chinese).
- Parsons MB, Azgaar AM, Curry JJ (1980). Hydrocarbon occurrences in the Sirte Basin, Libya. *CSPG Memoir* 6: 723–732.
- Peterson JA, Clarke JW (1983). Petroleum Geology and Resources of Volga-Urals Province, USSR. Alexandria, VC, USA: US Geological Survey.
- Proust JN, Chuvashov BI, Vennin E, Boisseau T (1998). Carbonate platform drowning in a foreland setting: the Mid-Carboniferous Platform in Western Urals (Russia). *J Sediment Res* 68: 1175–1188.
- Qin J, Ge L, Chen YM, Kang H, Liu Y (2011). Reservoir prediction of Lower Triassic Feixianguan Formation in Jiannan Area, Sichuan Basin. *Mar Origin Petrol Geol* 16: 9–17 (in Chinese).
- Sun ML, Liu GD, Li J (2008). Features of cap rocks of gas pools and criteria of identification. *Nat Gas Ind* 28: 36–38 (in Chinese).
- Tian NX, Chen WX, Huo H, Tian JB, Wu J (2008). Petroleum geology characteristics and play prediction in the Sirte Basin, Libya. *Oil Gas Geol* 29: 485–490 (in Chinese).
- Watts NL (1987). Theoretical aspects of cap-rock and fault seals for single and two-phase hydrocarbon columns. *Mar Petrol Geol* 4: 274–307.
- Wu GH, Chen ZY, Qu TL, Wang CH, Li HW, Zhu HY (2012). Characteristics of the strike-slip fault facies in Ordovician carbonate in the Tarim Basin, and its relations to hydrocarbon. *Acta Geol Sin* 86: 119–227 (in Chinese).
- Wu GH, Li QM, Zhang BS, Dong LS, Zhang YG, Zhang HQ (2005). Structural characteristics and exploration fields of No. 1 Faulted Slope Break in Tazhong area. *Acta Petrol Sin* 26: 27–30 (in Chinese).
- Xu ZY, Zhang GJ (2001). Divisional method and characteristic analysis of impermeable barrier layers in carbonate rock formation. *J China Univ Petrol*: 46–50 (in Chinese).

- Yang CZ, Zhang XP (1994). Relationship between dynamics of caprocks and characteristics of seal. *J SWPU* 16: 7–13 (in Chinese).
- Yang HJ, Wu GH, Han JF, Wang XF, Ji YG (2007). Characteristics of hydrocarbon enrichment along the Ordovician carbonate platform margin in the central uplift of Tarim Basin. *Acta Petrol Sin* 28: 26–31 (in Chinese).
- Yu LJ, Fan M, Liu WX, Zhang WT, Chen HY (2011). Seal mechanism of cap rocks. *Petrol Geol Exp* 33: 91–95 (in Chinese).
- Yuan SQ, Jia CZ, Gao RS, Pan WQ, Hou FD, Qi JH, Wu ZZ, Fa GF (2012). Sedimentation characteristics and reservoir geological model of Mid-Lower Ordovician carbonate rock in Tazhong northern slope. *Acta Petrolei Sin* 33: 80–88 (in Chinese).
- Zhang LH, Zhou GS (2010). Improvement and application of the methods of gas reservoir cap sealing ability. *Acta Sedimentol Sin* 28: 388–394 (in Chinese).
- Zhang LY, Bao YS, Liu Q, Zhang SC, Zhu RF, Zhang L (2010). Effects of hydrocarbon physical properties on caprock's capillary sealing ability. *Sci China Ser D* 40: 28–33 (in Chinese).
- Zhang QS (1998). Grey clustering evaluation method of the sealing ability of cap rock. *Petrol Explor Dev* 25: 34–36 (in Chinese).
- Zhou XY, Wang ZM, Yang HJ, Wang QH, Wu GH (2006). Tazhong Ordovician condensate field in Tarim Basin. *Mar Origin Petrol Geol* 11: 45–51 (in Chinese).